Geomicrobiology Journal
Publication details, including instructions for authors and subscription information:
http://www.tandfonline.com/loi/ugmb20

Uranium Redox Cycling in Sediment and Biomineral Systems

Gareth T. W. Law [a], Andrea Geissler [a], Ian T. Burke [b], Francis R. Livens [c], Jonathan R. Lloyd [a], Joyce M. McBeth [a] & Katherine Morris [a]

[a] Research Centre for Radwaste and Decommissioning and Williamson Research Centre for Molecular Environmental Science, School of Earth, Atmospheric and Environmental Sciences, The University of Manchester, Manchester, United Kingdom

[b] Earth System Science Institute, School of Earth and Environment, University of Leeds, Leeds, United Kingdom

[c] Centre for Radiochemistry Research, School of Chemistry, The University of Manchester, Manchester, United Kingdom

Available online: 26 Jul 2011

To cite this article: Gareth T. W. Law, Andrea Geissler, Ian T. Burke, Francis R. Livens, Jonathan R. Lloyd, Joyce M. McBeth & Katherine Morris (2011): Uranium Redox Cycling in Sediment and Biomineral Systems, Geomicrobiology Journal, 28:5-6, 497-506

To link to this article: http://dx.doi.org/10.1080/01490451.2010.512033

Geomicrobiology Journal, 28:497–506, 2011

ISSN: 0149-0451 print / 1521-0529 online
DOI: 10.1080/01490451.2010.512033

Taylor & Francis
Taylor & Francis Group

Uranium Redox Cycling in Sediment and Biomineral Systems

Gareth T. W. Law,[1] Andrea Geissler,[1] Ian T. Burke,[2] Francis R. Livens,[3] Jonathan R. Lloyd,[1] Joyce M. McBeth,[1] and Katherine Morris[1]

[1]*Research Centre for Radwaste and Decommissioning and Williamson Research Centre for Molecular Environmental Science, School of Earth, Atmospheric and Environmental Sciences, The University of Manchester, Manchester, United Kingdom*
[2]*Earth System Science Institute, School of Earth and Environment, University of Leeds, Leeds, United Kingdom*
[3]*Centre for Radiochemistry Research, School of Chemistry, The University of Manchester, Manchester, United Kingdom*

Under anaerobic conditions, uranium solubility is significantly controlled by the microbially mediated reduction of relatively soluble U(VI) to poorly soluble U(IV). However, the reaction mechanism(s) for bioreduction are complex with prior sorption of U(VI) to sediments significant in many systems, and both enzymatic and abiotic U(VI) reduction pathways potentially possible. Here, we describe results from sediment microcosm and Fe(II)-bearing biomineral experiments designed to assess the relative importance of enzymatic vs. abiotic U(VI) reduction mechanisms and the long-term fate of U(IV). In oxic sediments representative of the UK Sellafield reprocessing site, U(VI) was rapidly and significantly sorbed to surfaces and during microbially-mediated bioreduction, XAS analysis showed that sorbed U(VI) was reduced to U(IV) commensurate with Fe(III)-reduction. Additional control experiments with Fe(III)-reducing sediments that were sterilized after bioreduction and then exposed to U(VI), indicated that U(VI) reduction was inhibited, implying that enzymatic as opposed to abiotic mechanisms dominated in these systems. Further experiments with model Fe(II)-bearing biomineral phases (magnetite and vivianite) showed that significant U(VI) reduction occurred in co-precipitation systems, where U(VI) was spiked into the biomineral precursor phases prior to inoculation with *Geobacter sulfurreducens*. In contrast, when U(VI) was exposed to pre-formed, washed biominerals, XAS analysis indicated that U(VI) was recalcitrant to reduction. Re-oxidation experiments examined the long-term fate of U(IV). In sediments, air exposure resulted in Fe(II) oxidation and significant U(IV) oxidative remobilization. By contrast, only partial oxidation of U(IV) and no remobilization to solution occurred with nitrate mediated bio-oxidation of sediments. Magnetite was resistant to biooxidation with nitrate. On exposure to air, magnetite changed from black to brown in colour, yet there was limited mobilization of uranium to solution and XAS confirmed that U(IV) remained dominant in the oxidized mineral phase. Overall these results highlight the complexity of uranium biogeochemistry and highlight the importance of mechanistic insights into these reactions if optimal management of the global nuclear legacy is to occur.

Keywords uranium, sediment, bioreduction, biomineral, redox

INTRODUCTION

Uranium-238 is a long-lived ($^{238}U = 4.5 \times 10^9$ years) alpha-emitting-radionuclide that is present as a subsurface contaminant at nuclear legacy sites (Morris et al. 2002; Istok et al. 2004). In oxic environments, U(VI) dominates as the uranyl cation (UO_2^{2+}), which displays a range of environmental behaviors, ranging from being highly soluble in acidic or carbonate dominated environments (Lovley et al. 1992; Clark et al. 1995) to being extensively sorbed to geomedia in the absence of complexants (Sylwester et al. 2000; Barnett et al. 2002; Ortiz-Bernad et al. 2004; Jeon et al. 2005; Dong et al. 2006; Begg et al. 2010). Under anoxic conditions, highly insoluble $U(IV)O_2$ dominates speciation (Lovley et al. 1991; Lloyd and Renshaw 2005).

In axenic culture, microcosm, and *in situ* studies, microbially-mediated reduction has been shown to facilitate formation of insoluble U(IV) from both soluble and sorbed U(VI) (e.g., Lovley et al. 1991; Fredrickson et al. 2000; Finneran et al. 2002; Istok et al. 2004; Wilkins et al. 2007; Begg et al. 2010). Here, U(VI) is reduced to U(IV) commensurate with the development of Fe(III)- and/or sulfate-reducing conditions, with reduction facilitated via enzymatic processes and/or abiotic reaction with the reduced by-products of microbial metabolism (e.g., Fe(II)-biominerals). Indeed, in systems where U(VI) is partially

Received 21 April 2010; accepted 27 July 2010.

Current affiliation for A. Geissler: Forschungszentrum Dresden-Rossendorf, Dresden Germany

Current affiliation for J. M. McBeth: Bigelow Laboratory for Ocean Sciences, West Boothbay Harbour, Maine, USA

Address correspondence to Katherine Morris, Research Centre for Radwaste and Decommissioning and Williamson Research Centre for Molecular Environmental Science, School of Earth, Atmospheric and Environmental Sciences, The University of Manchester, Manchester, M13 9PL, United Kingdom. E-mail: kath.morris@manchester.ac.uk

soluble in groundwaters, 'biostimulation' of indigenous sediment bacteria to cause reduction of U(VI) has been suggested as an *in situ* remediation strategy for nuclear legacy sites (Lovley et al. 1991; Lloyd and Renshaw 2005).

However, as work prompted by an interest in U(VI) bioreduction has proceeded, the intricacy of uranium biogeochemistry has become apparent. For example, U(VI) can be recalcitrant to reduction in some systems (Ortiz-Bernad et al. 2004; Jeon et al. 2005) and easily reducible in others (Istok et al. 2004; Wilkins et al. 2007; Begg et al. 2010). Further, there is ongoing debate regarding the relative importance of enzymatic vs. abiotic reduction mechanisms in the environment (Fredrickson et al. 2000; Finneran et al. 2002; Anderson et al. 2003; Lloyd and Renshaw 2005; Liu et al. 2005; Behrends et al. 2005; Begg et al. 2010) and in this context there is also a paucity of information concerning uranium interactions with environmentally relevant Fe(II)-minerals, including biologically precipitated "biominerals" (Sharp et al. 2008; O'Loughlin et al. 2010).

The reoxidation behavior of U(IV) in environmental systems is also poorly characterized, with work to date showing variable rates of U(IV) oxidation and remobilization in the presence of the key oxidants air and nitrate (Moon et al. 2007; Wu et al. 2007; Komlos et al. 2008; Stewart et al. 2009; Begg et al. 2010). These results clearly demonstrate the complexity of uranium biogeochemistry in natural systems and highlight the importance of understanding uranium interactions with sediment and biomineral systems representative of the nuclear legacy. Here we investigated uranium biogeochemistry in: (i) progressively bioreduced and reoxidized sediments representative of the UK Sellafield nuclear facility; and (ii) environmentally relevant Fe(II)-bearing biominerals (magnetite (Fe_3O_4) and vivianite ($Fe_3(PO_4)_2 \cdot 8(H_2O)$)). Throughout, X-ray absorption spectroscopy (XAS) was used to characterize uranium solid-state interactions.

MATERIALS AND METHODS

Sample Collection

Sediments from the Quaternary unconsolidated alluvial flood-plain deposits known to underlie the Sellafield site (herein called Sellafield sediment) were collected from the Calder Valley, Cumbria, during September 2007. The sampling area was located ~2 km from the Sellafield site (Lat 54°26′30 N, Long 03°28′09 W). After sampling, sediments were transferred directly into a sterile HDPE sample container, sealed, and stored at 4°C in darkness. Experiments began within one month of sampling.

Sediment Bioreduction Microcosms

Sediment microcosms were prepared using a sediment and synthetic groundwater representative of the Sellafield region (Wilkins et al. 2007; Law et al. 2010). Previous experiments with these materials (Law et al. 2010) showed that the sediment was unable to support significant bioreduction without additional electron donor, thus 10 mM sodium acetate was added to the groundwater. The groundwater was sterilized by autoclaving (1 h at 120°C), sparged with filtered 80/20 N_2/CO_2, and pH adjusted to ~7.0 via addition of 0.01 M HCl. Sediments and groundwaters were then added to sterile glass serum bottles (Wheaton Scientific, USA) in a 1:20 ratio using aseptic technique, with the headspace purged with Ar prior to crimp sealing with butyl rubber stoppers.

Microcosms were then spiked to 105 μM $U(VI)O_2^{2+}$ (as uranyl chloride) via syringe addition. Sterile control experiments were established by autoclaving (3 × 20 min at 120°C over a one-week period) pre-prepared oxic microcosms and spiking with U(VI) via syringe addition. Groundwater only U(VI) amended microcosms were also established to monitor U(VI) solubility in the absence of sediments. All microcosms were incubated anaerobically at 21°C in the dark. Sediment slurry/groundwater was aseptically and sacrificially sampled in triplicate and both porewater and sediment samples were collected via centrifugation under an anoxic environment (15,000 *g*, 10 min). At each time point, one microcosm was frozen and stored at −80°C under argon for XAS analysis. Porewaters were sampled for U(VI), NO_3^-, NO_2^-, Fe, Mn, pH, and Eh and sediment samples were analyzed for 0.5 N HCl extractable Fe(II) and total Fe to estimate percentage Fe(III) reduction during anaerobic incubation. To further investigate U(VI) reduction mechanisms, U(VI) was added to pre-reduced Fe(III)-reducing sediments (>90% extractable Fe(II)) that were sterilized. This microcosm was then equilibrated for a further 10 days, geochemically sampled (as described previously), and frozen at −80°C under argon for XAS analysis.

Sediment Reoxidation Microcosms

Microbially active microcosms from the U(VI) bioreduction treatment that contained ≥90% extractable Fe(II) were uncapped and exposed to air with gentle agitation (O_2 oxidation) or injected with 25 mM $NaNO_3$ (nitrate oxidation). For nitrate reoxidation, a sterile control experiment was prepared by autoclaving a parallel U(VI) bioreduction microcosm prior to nitrate addition. Sampling of reoxidation microcosms followed bioreduction procedures (see above) and selected microcosm were frozen at −80°C under argon for XAS analysis (see next).

Biomineral Experiments

Interaction of U(VI) with biogenic magnetite and vivianite was also examined. Two experimental treatments were prepared for each mineral: (i) a co-precipitation treatment where U(VI) was added to the biomineral precursors prior to microbial inoculation; and (ii) a sorption treatment where U(VI) was reacted with pre-formed biogenic magnetite and vivianite. *Geobacter sulfurreducens* (strain ATCC 51573) was grown at 30°C under anaerobic conditions in an appropriate medium (Lovley and Phillips 1986) with acetate (20 mM) and fumerate (40 mM) as the electron donor and the electron acceptor, respectively, under an atmosphere of N_2-CO_2 (80:20). Late-log-phase

cultures were harvested by centrifugation at 4000 *g* for 10 min and washed twice in carbonate buffer ($NaHCO_3$ at 30 mM, pH 6.8) in N_2-CO_2 (80:20).

To produce magnetite, aliquots of the washed cell suspension (∼1 ml, final OD_{600} of ∼0.2) were added to anaerobic microcosms containing carbonate buffer (30 mM, pH 6.8), 50 mM ferric-gel (ferrihydrite) as the electron acceptor, and 20 mM acetate as an electron donor. For the co-precipitation treatment, 120 μM U(VI) was spiked and then incubated for ∼2 weeks at 30°C until magnetite formed. For the sorption treatment, the anaerobic microcosms containing *Geobacter* cells, bicarbonate, ferric-gel, and acetate were incubated for ∼2 weeks at 30°C until magnetite formed. The bio-precipitated magnetite (2.0 g) was sonicated, washed and resuspended in sterile groundwater in a 1:20 ratio, spiked with 105 μM U(VI) and left to equilibrate for 10 days prior to sampling. Biologically precipitated vivianite was prepared by adding an inoculum of *Geobacter sulfurreducens* cell suspension (∼1 ml to get a final OD_{600} of ∼0.2) to anaerobic microcosms containing an appropriate medium (Caccavo et al. 1994), with 56 mM ferric citrate as the electron accepter and 20 mM acetate as the electron donor.

For the co-precipitation treatment, 50 μM U(VI) was spiked into the microcosms which were then incubated for ∼4 weeks at 30°C until vivianite formed. For the sorption treatment, the bio-precipitated vivianite (1.0 g) was sonicated, washed, and resuspended in groundwater at a 1:20 ratio, spiked with 105 μM U(VI) and left to equilibrate for 10 days prior to sampling. During incubations, the aqueous phase (passed through a 0.22 μM filter) was sampled and analyzed for U(VI).

To further explore uranium reoxidation behavior, uranium amended magnetite from the co-precipitation treatment was reoxidized with air and nitrate. Here, the uranium labelled mineral phase was exposed to air with gentle agitation for 20 days or injected and incubated for 20 days with 25 mM nitrate and a 10% (vol:vol) inoculum of a stable consortium of nitrate-reducing Fe(II)-oxidizing bacteria (Morris et al. 2008). Selected samples from the sorption, co-precipitation, and reoxidation treatments were frozen at −80°C under argon for XAS analysis.

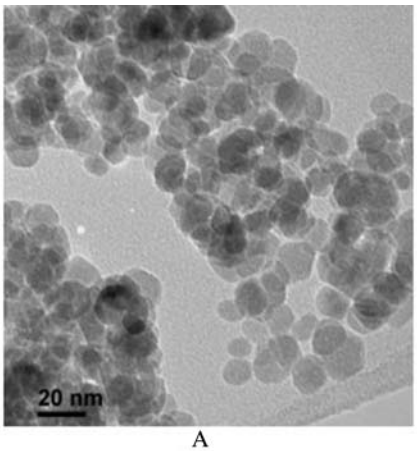

A

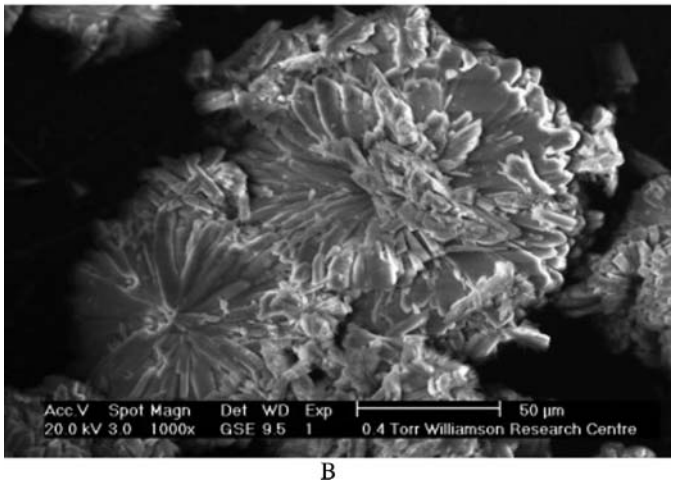

B

FIG. 1. Morphology of biominerals. (A) TEM image of magnetite; (B) ESEM image of vivianite. Scale bars are included on each image.

Geochemical Analyses

The mineral composition of the sediment and biomineral samples was quantified by X-ray diffraction and the sediment element composition was measured by X-ray fluorescence (Philips PW 1050 XRD, Thermo ARL 9400 XRF). The morphology of the biologically precipitated mineral phases was determined in analog experiments without added uranium by ESEM (Philips XL30 ESEM-FEG) and TEM (Phillips/FEI CM200). Total sediment organic content (TOC) was measured on a Carbo Erba EA12. Sediment colour was described using the Munsell Sediment Color Chart System (Munsell Color Company, USA) and sediment pH was determined according to Thomas, (1996). U(VI) and total Fe, Mn(II), and NO_2^- concentrations in porewaters were measured using UV-Vis spectroscopy methods on a Cecil CE 3021 spectrophotometer (Stookey, 1970; Johnson and Florence 1971; Brewer and Spencer 1971; Lovley and Phillips 1986; Viollier et al. 2000; Harris and Mortimer 2002). Aqueous NO_3^- and SO_4^{2-} were measured by ion chromatography. Total bioavailable Fe(III) and the proportion of extractable Fe(II) in the sediment was estimated by a 60 minute digestion of sediment in 0.5 N HCl (Lovley and Philips 1987). The pH and Eh were measured with an Orion 420A digital meter and calibrated electrodes. Standards were used routinely to check the reliability of all methods and calibration regressions had $R^2 \geq 0.99$.

X-Ray Absorption Spectrometry

To obtain information about the oxidation state of solid-phase associated uranium, key sediment and mineral treatments were selected for X-ray Absorption Near Edge Structure (XANES) analysis. Here, sediment or mineral phases that had been stored under argon at −80°C were thawed, separated by centrifugation (10 min; 4000 *g*) and the resultant solid pellet (moisture content < 50%) was triple contained in XAS

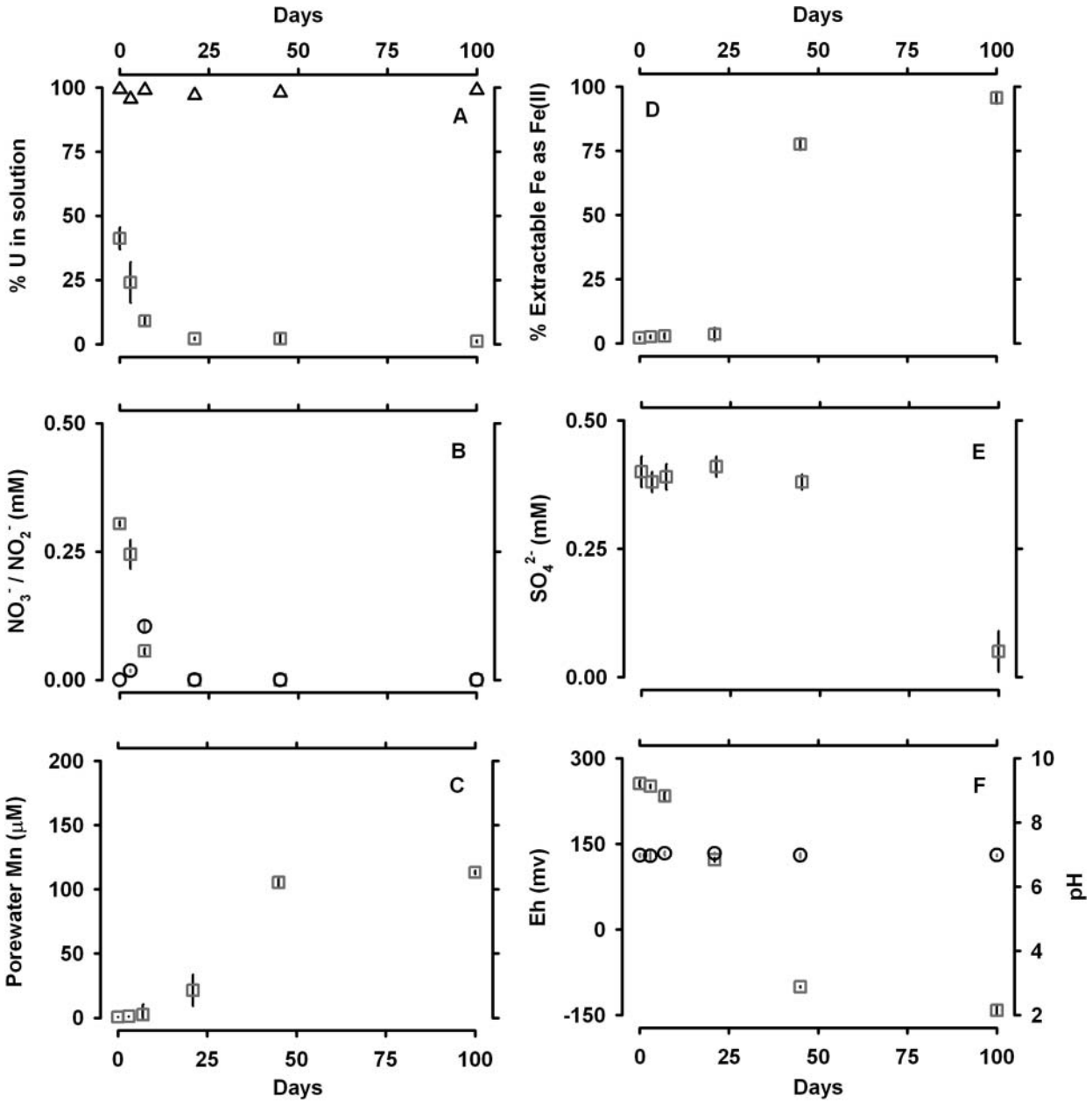

FIG. 2. Sediment microcosm bioreduction time-series data. (A) % U(VI) remaining in porewater (grey squares = microbially active sediments; black triangles = sterile groundwater no sediment); and in microbially active microcosms (B) NO_3^- (grey squares) and NO_2^- (black circles); (C) porewater Mn; (D) % extractable Fe as Fe(II); (E) porewater SO_4^{2-}; (F) porewater Eh (grey squares) and pH (black circles). Error bars represent 1 σ experimental uncertainty from triplicate microcosms (where not visible, error bars are within the symbol size).

sample cells in an anaerobic environment. Samples were then stored under argon at −80°C until XANES data acquisition. Both U(VI) (synthetic uranium trioxide; Strem Chemicals) and predominantly U(IV) (natural uraninite that contained minor U(VI) (Burns and Finch 1999)) solid phase standards were also prepared by dilution with boron nitride powder and transferred into triple contained cells for analysis.

Uranium L_{III}-edge spectra were collected at ambient temperature at the ultra-dilute spectroscopy line (16.5) at the UK CLRC Daresbury SRS, operating at 2 GeV with a typical current of 150 mA, using a Si(220) double crystal monochromator and unfocused optics. The incident beam intensity was detuned to 80% of maximum for harmonic rejection. Data for sediment and mineral samples were collected in fluorescence mode with a Canberra 30-element solid state Ge detector. Data for the U(VI) standard and U(IV)-bearing uraninite were collected in transmission mode using two ion chambers.

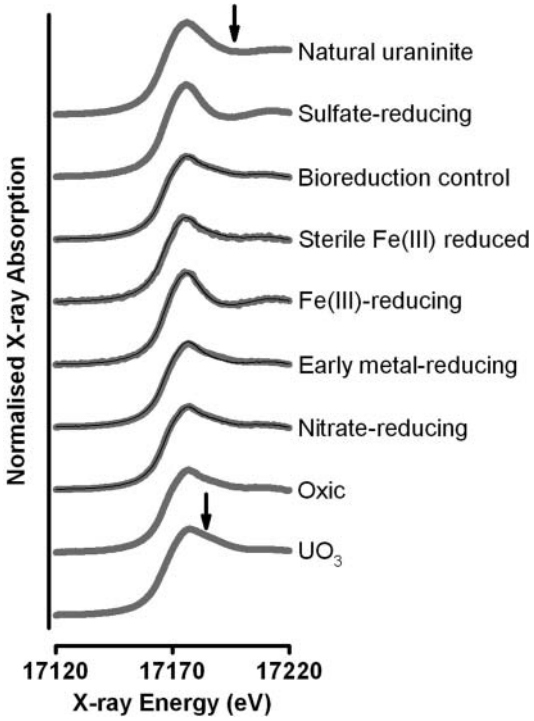

FIG. 3. Uranium L_{III}-edge XANES spectra for synthetic U(VI)O_3 and predominantly U(IV) natural uraninite oxidation standards diluted in boron nitride (grey lines) and corresponding linear combination fits (black lines) for uranium amended sediments under different bio-reducing conditions. Arrows indicates the position of diagnostic U(VI) post absorption edge spectral feature associated with the uranyl axial oxygens and the position of the U(IV) post absorption edge trough.

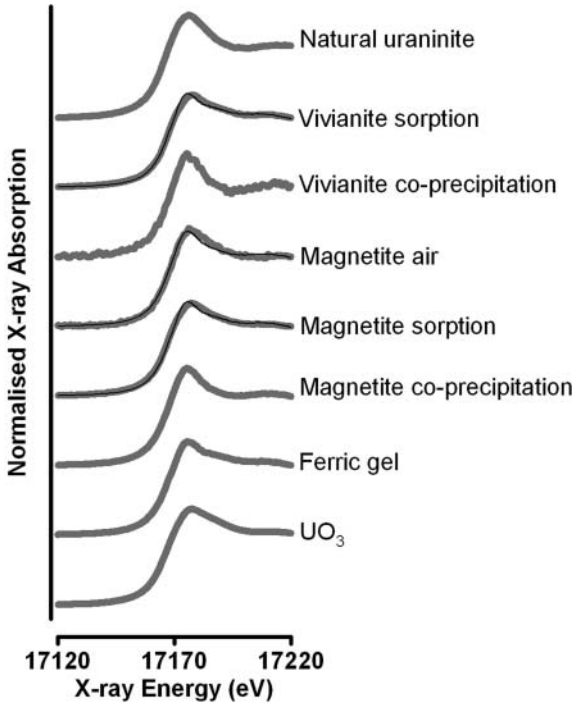

FIG. 4. Uranium L_{III}-edge XANES spectra for synthetic U(VI)O_3 and predominantly U(IV) natural uraninite oxidation standards diluted in boron nitride and spectra (grey lines) and corresponding linear combination fits (black lines) for ferric gel and Fe(II) biominerals from the co-precipitation and sorption treatments.

XANES Analysis

XANES spectra from all samples were calibrated, background subtracted, and normalised for drift to a standardised E_0 position. The XANES spectra from end-member sediment redox states (oxic and sulfate reduced samples) and end-member mineral samples (ferric gel and co-precipitated magnetite and vivianite) were then compared to the U(VI)- and uraninite-standard spectra (Figure 3) and literature examples (e.g., O'Loughlin et al. 2003; Wu et al. 2010). This comparison revealed that within the expected spectral differences apparent between non-matrix matched systems, the oxic sediment and ferric gel displayed U(VI)-like XANES, and the sulfate-reduced sediment and co-precipitated magnetite and vivianite displayed U(IV)-like XANES (Figures 3 and 4).

To gain insight into the extent and timing of U(VI) reduction in these systems, the ATHENA linear combination fitting (LCF) routine (Ravel and Newville 2005) was used to quantify the contributions of the different end-member spectra to the remaining sediment and mineral spectra. Specifically, linear combination fitting was conducted for sediments using (i) oxic (U(VI)) and (ii) sulfate-reduced (~U(IV)) sediment end-member spectra, and for minerals (i) ferric gel (U(VI)) and (ii) co-precipitated magnetite/vivianite (~U(IV)) end-member spectra.

RESULTS AND DISCUSSION

Sediment Characteristics

The sediment mineral content was dominated by quartz, sheet silicates (muscovite and chlorite), and feldspars (albite and microcline). The elemental composition was dominated by Si (34.0 wt %), with significant concentrations of Al (5.8 wt %), Fe (3.1 wt %), Ca (0.2 wt %), Na (1.0 wt %), Mg (0.53 wt %), and Mn (0.1 wt %) also present. The air-dried sediment was red in colour (Munsell notation of 2.5YR 4/8) and the sediment had an approximate particle composition of 53% sand, 42% silt, and 5% clay, a pH of 5.5, and a TOC content of 0.56 ± 0.08 wt %.

Mineral Characteristics

Characterisation of minerals using XRD indicated that the ferric gel was ferrihydrite and the Fe(II)-bearing biomineral preparations were predominantly magnetite and vivianite. Biomineral morphology was also examined in analog experiments using ESEM and TEM (Figure 1). Black magnetite grains (~30 nm in diameter, Figure 1A) formed aggregates of ~40–200 nm diameter. White vivianite crystals (Figure 1B) formed radiating rosettes with thin blades of ~20–40 μm in length and ~5–10 μm width.

TABLE 1
Sediment microcosm characteristics during bioreduction (top) and reoxidation (bottom) with corresponding solid-phase uranium L_{III} edge XANES linear combination fitting (LCF) results

Sample	% 0.5 N extractable Fe(II)	% U(VI)(aq)	XANES linear combination modelling	
			% spectrum 1	% spectrum 2
Sulfate-reducing (100 days)	96	2	-	-
Sterile Fe(III) reduced (10 day exposure)	92	5	18	82
Fe(III)-reducing (45 days)	77	2	95	5
Early metal-reducing (21 days)	5	5	25	75
Nitrate-reducing (3 days)	3	24	3	97
Sterile oxic (bioreduction control) (100 days)	1	8	7	93
Oxic (1 hour)	2	40	-	-
Air oxidized (1 day)	2	92	*	*
Nitrate oxidized (20 days)	19	3	64	36
Nitrate oxidized (5 days)	70	3	73	27
Nitrate amended sterile control (20 days)	94	2	83	17

LCF fitting errors were estimated to be ± ∼15%. End-member spectra used in linear combination modelling (denoted by (-) symbol) were (spectrum 1) U(IV) sorbed to sulfate-reducing sediments, and (spectrum 2) U(VI) sorbed to oxic sediment. *XANES data not collected as uranium concentration was too low.

Uranium Adsorption and Progressive Bioreduction in Sediment Microcosms

To investigate uranium behavior in oxic groundwater and Sellafield sediment/groundwater systems, U(VI) was added to sterilized oxic groundwater, sterilized sediment slurry, and microbially-active sediment slurry microcosms. In the sterile groundwater system, U(VI) remained in solution throughout the incubation and was undersaturated (Figure 2A). In the sterile sediment system, U(VI) was significantly sorbed to surfaces, with >90% of the U(VI) spike associated with the sediments after 100 days (Table 1), presumably reflecting rapid reaction of U(VI) with surface sites followed by structural rearrangement of the UO_2^{2+} moiety on active surfaces (Barnett et al. 2002; Cheng et al. 2006; Dong et al. 2006; Um et al. 2007; Begg et al. 2010). There was no evidence for bioreduction in this sample.

In the microbially active sediment system, >60% of the added U(VI) was sorbed to the sediments under oxic conditions after 1 h (Figure 2A). Thereafter, bioreduction proceeded, with terminal electron accepting processes (TEAPs) progressing via: denitrification (indicated by removal of NO_3^- and NO_2^- between days 0–21 (Figure 2B)); early metal reduction (indicated by Mn(II) production to pore waters (Figure 2C) and <10% Fe(II) in sediments (Figure 2D) between days 7–21); Fe(III) reduction (indicated by Fe(II) in sediments >10% after 21 days (Figure 2D)); and sulfate reduction (indicated by >75% extractable Fe present as Fe(II), black sediment, and removal of porewater SO_4^{2-} after 45 days (Figure 2E)). Progression of these TEAPs was largely complete by 100 days (Figure 2). During bioreduction, porewater pH remained constant at ∼7.0 (Figure 2F), Eh tracked the dominant TEAPs (Figure 2F), and porewater U(VI) concentrations were <5% after 21 days (Figure 2A).

Uranium Solid-Phase Interaction During Progressive Bioreduction

As uranium was rapidly sorbed to the sediments, X-ray absorption spectroscopy was used to track uranium behavior during TEAP development. XANES spectra of solid-phase oxidation state standards (Figure 3) show that after the absorption edge: (i) U(VI) is dominated by a "flat" post-edge feature, due to the axial oxygen atoms in the uranyl moiety, and (ii) U(IV) is dominated by defined post-edge trough. In the sediment microcosms, XANES spectra for the oxic and denitrifying sediments had a similar shape to the U(VI) standard, indicating that sediment associated U(VI) dominates under these TEAPs (Figure 3).

By contrast, the early metal-reducing XANES spectrum was intermediate between the U(VI) and U(IV) standard spectra, whilst the Fe(III)- and sulfate-reducing spectra were similar in shape to the predominantly U(IV) natural uraninite standard, indicating bioreduction of sorbed U(VI) to U(IV) under prolonged metal- and/or sulfate-reducing conditions. Linear combination fitting between redox state end-member spectra (see methods for detail) supported these interpretations, with a U(VI) dominated spectrum in the nitrate-reducing system, and U(IV) becoming increasingly dominant during early metal, Fe(III), and sulfate reduction (Table 1).

Uranium Bioreduction Mechanisms

U(VI) reduction occurred during progressive anoxia, predominantly during microbially-mediated Fe(III) reduction

TABLE 2
U(VI) in solution and solid-phase uranium L_{III} edge XANES linear combination fitting results for biomineral reduction and reoxidation experiments

		XANES linear combination modelling	
Sample	% U(VI)(aq)	% spectrum 1	% spectrum 2
Ferric gel	~0	-	-
Magnetite co-precipitation	~0	-	-
Magnetite co-precipitation air (20 days)	2	52†	48†
Magnetite sorption (10 days exposure)	~0	10†	90†
Vivianite co-precipitation	~0	-	-
Vivianite sorption (10 days exposure)	~0	5‡	95‡

Linear combination fitting (LCF) errors were estimated to be +/− ~15%. End-member spectra used in linear combination modelling (denoted by (-) symbol) were (spectrum 1) U(IV) sorbed to "co-precipitated" magnetite† or vivianite‡, and (spectrum 2) U(VI) sorbed to ferric gel.

(Figure 3, Table 1). To assess the mechanism of bioreduction (i.e. enzymatic vs. abiotic), a control experiment was conducted. Here, sterile Fe(III)-reduced sediment was spiked with U(VI) and left to equilibrate for 10 days (Table 1). The XANES spectra and linear combination fitting of the sample indicated a predominantly U(VI)-like environment (Figure 3; Table 1), indicating that U(VI) reduction in this system may be primarily facilitated via enzymatic processes. Alternatively, changes in the physicochemical conditions of the sediments after autoclaving may have altered the U(VI) reduction potential. Regardless, these results are similar to findings for sediments from a range of nuclear legacy sites and suggest that under certain environmental conditions, U(VI) reduction is dominated by enzymatic pathways (Liu et al. 2005; Fox et al. 2006; Wilkins et al. 2007; Begg et al. 2010).

Uranium Interaction with Fe(II)-Bearing Biominerals

Whilst enzymatic reduction appears to dominate U(VI) reduction in Sellafield sediments, reduction in other systems has been attributed to U(VI) reaction with Fe(II)-bearing mineral phases and/or Fe(II) sorbed to surfaces (i.e., abiotic U(VI) reduction) (Moyes et al. 2000; Fredrickson et al. 2000; Misanna et al. 2003; Scott et al. 2005; Behrends et al. 2005; Jeon et al. 2005; O'Loughlin et al. 2003, 2010; Sharp et al. 2008; Ithurbide et al. 2009). This apparent inconsistency may reflect U(VI) specificity for differing Fe(II) phases, variation in the reactivity of different Fe(II) minerals, or differences in the reactivity of synthetic vs. biogenic Fe(II) minerals due to, for example, surface area or pH/surface speciation effects (Boyanov et al. 2007).

To further assess whether environmentally relevant Fe(II)-bearing biominerals can reduce U(VI), uranium interactions with model biogenic Fe(II)-bearing biominerals (magnetite and vivianite) were investigated. Two experimental treatments were undertaken: (i) co-precipitation, where U(VI) was added to magnetite and vivianite precursors prior to inoculation with *Geobacter sulfurreducens* and biomineral formation; and (ii) sorption, where U(VI) was spiked into the preformed, washed biomineral phases. In the co-precipitation treatments, uranium remained soluble in the Fe(III)-citrate medium used to prepare vivianite, but was completely sorbed to ferric gel (which was bioreduced to magnetite) as U(VI) (Figure 4). After magnetite and vivianite formation, all of the added uranium was sorbed to the mineral phases, with uranium XANES spectra reflecting a predominantly U(IV)-like environment (Figure 4).

In the sorption treatments, U(VI) removal was also marked, with ~90% of the added uranium sorbed to each mineral phase after 1 h, and ~100% sorbed after 2 days (Table 2). However, after 10 days equilibration, the XANES spectra were predominantly U(VI), with linear combination fitting suggesting that ≤10% of the uranium was present as U(IV) in the magnetite and vivianite samples (Figure 4; Table 2). When considered alongside the co-precipitation mineral and sediment data (Figures 3 and 4), these results highlight that U(VI) reduction is dominated by enzymatic pathways in these systems and further imply that biogenic magnetite and vivianite are ineffectual U(VI) reductants under the conditions of study.

These results are similar to past work (Moyes et al. 2000; Jeon et al. 2005; Ithurbide et al. 2009; O'Loughlin et al. 2010; Finneran et al. 2002) but contrast with the observations of several workers who have reported significant U(VI) reduction on exposure to synthetic and biogenic Fe(II)-bearing mineral phases (Misanna et al. 2003; Scott et al. 2005; Behrends et al. 2005; Boyanov et al. 2007; O'Loughlin et al. 2003, 2010; Sharp et al. 2008). Overall, it is clear that the key factors that control whether electron transfer to U(VI) can occur in the presence of Fe(II)-bearing mineral phases are highly specific to the conditions of study, and that under the ambient conditions studied here in both sediments and model mineral phases, enzymatic processes appear to enhance the extent of U(VI) reduction.

Uranium Reoxidation Behavior in Sediment Systems

To understand the long-term fate of bioreduced U(IV), we examined uranium behavior during air and nitrate reoxidation of Fe(III)-reducing, U(IV) labelled sediments. Air reoxidation resulted in rapid Fe(II) oxidation and almost complete uranium remobilization to solution as U(VI) within 24 hours (Table 1).

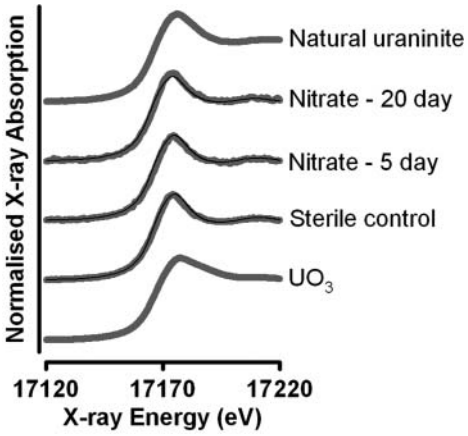

FIG. 5. Uranium L_{III}-edge XANES spectra for synthetic U(VI)O_3 and predominantly U(IV) natural uraninite oxidation standards diluted in boron nitride and spectra (grey lines) and corresponding linear combination fits (black lines) for sediments undergoing nitrate reoxidation.

This represents a profound change in the geochemistry of uranium in the system: initially, U(VI) was extensively sorbed to oxic sediments; during bioreduction, sorbed U(VI) was reduced to highly insoluble U(IV) under Fe(III)-reducing conditions; upon air reoxidation U(IV) was reoxidized and significantly remobilized to solution.

Similar results have been presented in other sediment systems (Moon 2007; Komlos et al. 2008) and the fast and complete oxidative remobilization of U(IV) indicates that either the Fe(III) phases formed during the oxidation of reduced sediments do not necessarily provide significant or suitable surfaces for U(VI) sorption or that U(VI) solubility increases due to changes in solution chemistry during reoxidation. Upon nitrate reoxidation, oxidation to Fe(III), significant gas production (presumably N_2), and transient NO_2^- production (data not shown) all indicated that Fe(II) oxidation was coupled to microbially mediated NO_3^- reduction (Table 1; Geissler et al. 2011, this issue).

However, in contrast to the air reoxidation system, U(IV) oxidation and remobilization was not as marked in this system, and after 20 days XANES analysis and linear combination fitting highlighted that ~64% of U(IV) remained in the sediment despite >80% of extractable Fe being present as Fe(III) (Figure 5, Table 1). These results contrast with other studies that have found that nitrate and the by-products of nitrate reduction (e.g., NO_2^-, N_2O) are efficient U(IV) oxidants (e.g., Senko et al. 2002; Moon et al. 2007). Ultimately, these observations highlight that the long-term fate of U(IV) is intimately linked to sediment Fe mineralogy, oxidant type, and solution chemistry, with the factors controlling the redox biogeochemistry of U(IV) in complex environments warranting further study.

Uranium Reoxidation Behavior in Mineral Systems

To further explore uranium behavior in model mineral systems undergoing reoxidation, co-precipitated magnetite was treated with air and nitrate. Monitoring the reoxidation biogeochemistry of these systems proved to be challenging as 0.5 N HCl was an ineffectual lixivant for the mineral phase. Regardless, there was a clear colour change on air reoxidation, with the black magnetite forming a dark brown mineral phase. In this system, uranium remained sorbed to the reoxidized solid phase and XANES analysis with linear combination fitting between ferricgel (U(VI)) and co-precipitated magnetite(~U(IV)) showed that uranium speciation in the reoxidized phase was mixed (Figure 4, Table 2). Similar results have been presented for other Fe(II)/Fe(III)-bearing phases undergoing redox cycling (Stewart et al. 2009). Interestingly, microbially-mediated nitrate reoxidation of magnetite proved to be ineffectual and there was no visual evidence for Fe(III) formation with time. Overall, these results highlight that air can partially reoxidize U(IV) sorbed to magnetite, with the resultant Fe(III)-bearing mineral phase remaining as an effective sorbent for resulting U(VI).

Summary

These data provide evidence that enzymatic processes dominate U(VI) bioreduction in heterogeneous sediment systems and select model mineral systems under the conditions and timeframes of study. The results also emphasise the complexity of the redox cycling processes and their effects on bioreduced uranium, with U(IV) displaying variable rates of oxidation upon exposure to air or nitrate, and mineralogical changes in the sediment potentially affecting U(VI) sorption potential. These observations have significant implications for contaminated land and geological disposal scenarios where bioreduction may enhance uranium retention within the geosphere and highlight the need for the site specific evaluation and optimisation of any biostimulation strategy.

ACKNOWLEDGMENTS

We thank Rob Mortimer, Lesley Neve, James Begg, and Dave Hatfield (University of Leeds), Bob Bilsborrow (SRS Daresbury), and Christopher Boothman (University of Manchester) for help with data acquisition, and Vicky Coker (University of Manchester) and Mike Kelly (University of Leeds) for ESEM and TEM images. This work was supported by the UK Natural Environment Research Council (NERC) grants (NE/D00473X/1 & NE/D005361/1) and by STFC beam-time awards at SRS Daresbury.

REFERENCES

Anderson RT, Vrionis HA, Ortiz-Bernad I, Resch CT, Long PE, Dayvault R, Karp K, Marutzky S, Metzler DR, Peacock A, White DC, Lowe M, Lovley DR. 2003. Stimulating the in situ activity of *Geobacter* species to remove uranium from the groundwater of a uranium-contaminated aquifer. Appl Environ Microbiol 69:5884–5891.

Barnett MO, Jardine PM, Brooks SC. 2002. U(VI) adsorption to heterogeneous subsurface media: application of a surface complexation model. Environ Sci Technol 36:937–942.

Begg JDC, Burke ITB, Lloyd IT, Boothman CB, Shaw S, Charnock JM, Morris K. 2011. Bioreduction behavior of U(VI) sorbed to sediments. Geomicrobiol J 28:160–171.

Behrends T, Van Cappellen P. 2005. Competition between enzymatic and abiotic reduction of uranium(VI) under iron reducing conditions. Chem Geol 220:315–327.

Boyanov M, O'Loughlin EJ, Roden E, Fein J, Kemner K. 2007. Adsorption of iron(II) and uranium(VI) to carboxyl-functionalized microspheres: the influence of speciation on uranyl reduction studied by titration and XAFS. Geochim Cosmochim Acta 71:1898–1912.

Brewer PG, Spencer DW. 1971. Colourimetric determination of Mn in anoxic waters. Limnol Oceanogr 16:107–110.

Burns PC, Finch R. 1999. Uranium: mineralogy, geochemistry and the environment. Rev Mineral 38:1–679.

Caccavo JR, Lonergan DJ, Lovley DR, Davis M, Stolz JF, McInerney MJ. 1994. *Geobacter sulfureducens* sp. nov., a hydrogen- and acetate-oxidizing dissimilatory metal-reducing microorganism. Appl Environ Microbiol 60:3752–3759.

Cheng T, Barnett MO, Roden EE, Zhuang J. 2006. Effects of solid-solution ratio on uranium(VI) adsorption and its implications. Environ Sci Technol 40:3243–3247.

Clark DL, Hobart DE, Neu MP. 1995. Actinide carbonate complexes and their importance in actinide environmental chemistry. Chem Rev 95:25–48.

Coppi MV, Leang C, Sandler SJ, Lovley DR. 2001. Development of a genetic system for *Geobacter sulfurreducens*. Appl Environ Microbiol 67:3180–3187.

Dong W, Xie G, Miller TR, Franklin MP, Oxenberg TP, Bouwer EJ, Ball WP, Halden RU. 2006. Sorption and bioreduction of hexavalent uranium at a military facility by the Chesapeake Bay. Environ Pollut 142:132–142.

Finneran KT, Anderson RT, Nevin KP, Lovley DR. 2002. Potential for bioremediation of uranium-contaminated aquifers with microbial U(VI) reduction. Soil Sed Contam 11:339–357.

Fox JR, Mortimer RJG, Lear G, Lloyd JR, Beadle I, Morris K. (2006) The biogeochemical behavior of U(VI) in the simulated near-field of a low-level radioactive waste repository, Appl Geochem 21:1539–1550.

Fredrickson JK, Zachara JM, Kennedy DW, Duff MC, Gorby YA, Li SW, Krupka M. 2000. Reduction of U(VI) in goethite ([alpha]-FeOOH) suspensions by a dissimilatory metal-reducing bacterium. Geochim Cosmochim Acta 64:3085–3098.

Geissler A, Law GTW, Morris K, Boothman C, Burke ITB, Livens FR, Lloyd JR. 2011. (this issue). Microbial communities associated with the oxidation of iron and technetium in bioreduced sediments.

Harris SJ, Mortimer RJG. 2002. Determination of nitrate in small water samples (100 μL) by the cadmium-copper reduction method: A manual technique with application to the interstitial waters of marine sediments. Int J Environ Anal Chem 82:369–376.

Istok JD, Senko JM, Krumholz LR, Watson D, Bogle MA, Peacock A, Chang YJ, White DC. 2004. *In situ* bioreduction of technetium and uranium in a nitrate-contaminated aquifer. Environ Sci Technol 38:468–475.

Ithurbide A, Peulon S, Miserque F, Beaucaire C, Chausse C. 2009. Interaction between uranium (VI) and siderite in carbonate solutions. Radiochim Acta 97:177–180.

Jeon BH, Dempsey BA, Burgos WD, Barnett MO, Roden EE. 2005. Chemical reduction of U(VI) by Fe(II) at the solid-water interface using natural and synthetic Fe(III) oxides. Environ Sci Technol 39:5642–5649.

Johnson DA, Florence TM. 1971. Spectrophotometric determination of uranium(VI) with 2-(5-bromo-2-pyridylazo)-5diethylaminophenol. Anal Chim Acta 53:73–79.

Komlos J, Peacock A, Kukkadapu RK, Jaffé PR. 2008. Long-term dynamics of uranium reduction/reoxidation under low sulfate conditions. Geochim Cosmochim Acta 72:3603–3615.

Law GTW, Geissler A, Boothman C, Burke IT, Livens FR, Lloyd JR, Morris K. 2010. Role of nitrate in conditioning aquifer sediments for technetium bioreduction. Environ Sci Technol 44:150–155.

Liu C, Zachara JM, Zhong L, Kukkadupa R, Szecsody JE, Kennedy DW. 2005. Influence of sediment bioreduction and reoxidation on uranium sorption. Environ Sci Technol 39:4125–4133.

Lloyd JR, Renshaw JC. 2005. Bioremediation of radioactive waste: radionuclide-microbe interactions in laboratory and field-scale studies. Curr Opin Biotech 16:254–260.

Lovley DR, Phillips EJP. 1986. Availability of ferric iron for microbial reduction in bottom sediments of the freshwater tidal Potomac River. Appl Environ Microbiol 52:751–757.

Lovley DR, Phillips EJP. 1987. Rapid assay for microbially reducible ferric iron in aquatic sediments. Appl Environ Microbiol 53:1536–1540.

Lovley DR, Phillips EJP, Gorby YA, Landa ER. 1991. Microbial reduction of uranium. Nature 350:413–416.

Lovley DR, Philips EJP. 1992. Reduction of uranium by *Desulfovibrio desulfuricans*. Appl Environ Micro 58:850–856.

Missana T, Maffiotte C, García-Gutiérrez M. 2003, Surface reactions kinetics between nanocrystalline magnetite and uranyl. J Coll Interf Sci 261:154–160.

Moon HS, Komlos J, Jaffé PR. 2007. Uranium reoxidation in previously bioreduced sediment by dissolved oxygen and nitrate. Environ Sci Technol 41:4587–4592.

Morris K, Raiswell R. 2002. Biogeochemical cycles and the remobilization of the actinide elements. In: Interactions of Microorganisms with radionuclides, Keith-Roach MJ, Livens FR, editors. Elsevier, London.

Morris K, Livens FR, Charnock JM, Burke IT, McBeth JM, Begg JDC, Boothman C, Lloyd JR. 2008. An X-ray absorption study of the fate of technetium in reduced and reoxidized sediments and mineral phases. Appl Geochem 23:603–617.

Moyes LN, Parkman RH, Charnock JM, Vaughan DJ, Livens FR, Hughes CR, Braithwaite A. 2000. Uranium uptake from aqueous solution by interaction with goethite, lepidocrocite, muscovite, and mackinawite: an X-ray absorption spectroscopy study. Environ Sci Technol. 34:1062–1068.

O'Loughlin EJ, Kelly SD, Cook RE, Csencsits R, Kemner KM. 2003. Reduction of uranium(VI) by mixed iron(II)/iron(III) hydroxide (green rust): formation of UO_2 nanoparticles. Environ Sci Technol 37:721–727.

O'Loughlin EJ, Kelly SD, Kemner KM. 2010. XAFS investigation of the interactions of U(VI) with secondary mineralization products from the bioreduction of Fe(III) oxides. Environ Sci Technol 44:1656–1661.

Ortiz-Bernad I, Anderson RT, Vrionis HA, Lovley DR. 2004. Resistance of solid-phase U(VI) to microbial reduction during in situ bioremediation of uranium-contaminated groundwater. Appl Environ Microbiol 70:7558–7560.

Ravel B, Newville M. 2005. ATHENA, ARTEMIS, HEPHAESTUS: Data analysis for X-ray absorption spectroscopy using IFEFFIT. J Synchrotron Rad 12:537–541.

Scott TB, Allen GC, Heard PJ, Randell MG. 2005. Reduction of U(VI) to U(IV) on the surface of magnetite. Geochim Cosmochim Acta 69:5639–5646.

Senko JM, Istok JD, Suflita JM, Krumholz LR. 2002. *In situ* evidence for uranium immobilization and remobilization. Environ Sci Technol 36:1491–1496.

Sharp JO, Schofield E, Veeramani H, Suvorova E, Junier P, Bargar JR, Bernier-Latmani R. 2008. Uranyl reduction by *Geobacter sulfurreducens* in the presence or absence of iron. In: Merkel BJ, Hasche-Berger A, editors. Uranium, Mining and Hydrogeology. Springer: Berlin. P 725–732.

Stewart BD, Nico PS, Fendorf S. 2009. Stability of uranium incorporated into Fe (hydr)oxides under fluctuating redox conditions. Environ Sci Technol 4:4922–4927.

Stookey LL. 1970. Ferrozine—A new spectrophotometric reagent for iron. Anal Chem 42:779–781.

Sylwester ER, Hudson EA, Allen PG. 2000. The structure of uranium (VI) sorption complexes on silica, alumina, and montmorillonite. Geochim Cosmochim Acta 64:2431–2438.

Thomas GW. 1996. Soil pH and acidity. In: Sparks D, editor. Methods of Soil Analysis, Part 3—Chemical Methods. Madison, WI: Soil Science Society of America.

Um W, Serne RJ, Krupka KM. 2007. Surface complexation modeling of U(VI) sorption to Hanford sediment with varying geochemical conditions. Environ Sci Technol 41:3587–3592.

Viollier E, Inglett PW, Hunter K, Roychoudhury AN, Van Cappellen P. 2000. The ferrozine method revisited: Fe(II)/Fe(III) determination in natural waters. Appl Geochem 15:785–790.

Wilkins MJ, Livens FR, Vaughan DJ, Beadle I, Lloyd JR. 2007. The influence of microbial redox cycling on radionuclide mobility in the subsurface at a low-level radioactive waste storage site. Geobiology 5:293–301.

Wu WM, Carley J, Luo J, Ginder-Vogel MA, Cardenas E, Leigh MB, Hwang CC, Kelly SD, Ruan CM, Wu LY, Van Nostrand J, Gentry T, Lowe K, Mehlhorn T, Carroll S, Luo WS, Fields MW, Gu BH, Watson D, Kemner KM, Marsh T, Tiedje J, Zhou JZ, Fendorf S, Kitanidis PK, Jardine PM, Criddle CS. 2007. In situ bioreduction of uranium (VI) to submicromolar levels and reoxidation by dissolved oxygen. Environ. Sci. Technol. 41:5716–5723.

Wu WM, Carley J, Green SJ, Luo J, Kelly SD, Van Nostrand J, Lowe K, Mehlhorn T, Carroll S, Boonchayanant B, Löfller FE, Watson D, Kemner KM, Zhou J, Kitanidis PK, Kostka JE, Jardine PM, Criddle CS. 2010. Effects of nitrate on the stability of uranium in a bioreduced region of the subsurface. Environ Sci Technol 44:5104–5111.